



Supplement of

An integrated analysis of contemporary methane emissions and concentration trends over China using in situ and satellite observations and model simulations

Haiyue Tan et al.

Correspondence to: Lin Zhang (zhanglg@pku.edu.cn)

The copyright of individual parts of the supplement might differ from the article licence.

Table S1. Global CH₄ sources and sinks (Tg CH₄ a⁻¹) in the 2000s and 2010s. Our results with the EDGAR inventory (GCE) and the CEDS inventory (GCC) are compared with values summarized by Saunois et al. (2020).^a

Time period	Saunois et al. (2020)				This study			
	2000–2009		2008–2017		2000–2009		2008–2017	
Approach ¹	B-U	T-D	B-U	T-D	GCE	GCC	GCE	GCC
Anthropogenic sources	334 (321–358)	332 (312–347)	366 (349–393)	359 (336–376)	327	340	362	380
Agriculture and waste	192 (178–206)	202 (198–219)	206 (191–223)	217 (207–240)	205	186	220	200
Biomass and biofuel burning	31 (26–46)	29 (23–35)	30 (26–40)	30 (22–36)	26	25	29	27
Fossil fuels	110 (94–129)	101 (71–151)	128 (113–154)	111 (81–131)	94	129	112	153
Natural sources	369 (245–485)	215 (176–243)	371 (245–488)	218 (183–248)	193		194	
Wetlands	147 (102–179)	180 (153–196)	149 (102–182)	181 (159–200)	177		177	
Other sources	222 (143–306)	35 (21–47)	222 (143–306)	37 (21–50)	17		17	
Sinks								
Soils	30 (11–49)	34 (27–41)	30 (11–49)	38 (27–45)	18		18	
Total chemical loss	595 (489–749)	505 (459–516)	595 (489–749)	518 (474–532)	494	501	519	535
Totals								
Sum of sources	703 (566–842)	547 (524–560)	737 (594–881)	576 (550–594)	520	533	556	574
Sum of sinks	625 (500–798)	540 (486–556)	625 (500–798)	556 (501–574)	512	519	537	553
Imbalance	78	3 (–10–38)	112	13 (0–49)	8	14	19	21

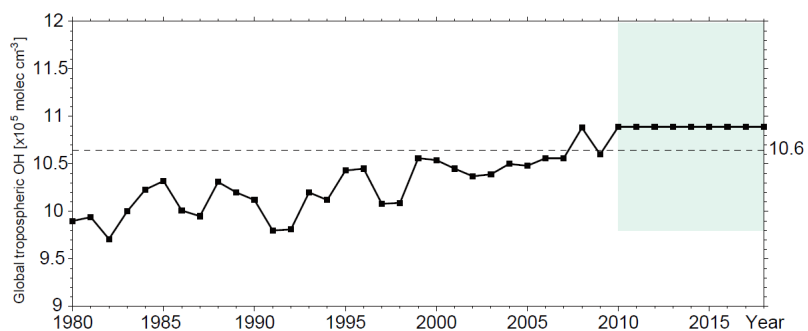
^a Values are estimated by the bottom-up (B-U) and top-down (T-D) approaches, and from our GCC and GCE simulations. Values from Saunois et al. (2020) are presented as means and ranges (minimum and maximum). Rounding errors may result in 1 Tg CH₄ a⁻¹ differences in the totals.

10 Table S2. Main categories of CH₄ sources and sinks in GCE and GCC

Sectors		GCE	GCC
Sources	Agriculture and waste (AW)	Enteric fermentation & Manure management (LIV)	Non-combustion agricultural sector (AGR)
		Rice cultivation (RIC)	
		Waste water handling (WST)	Waste disposal and handling (WST)
		Solid waste landfills (LDF)	
	Solid waste incineration		
	Biomass and biofuel burning (BB)	Biomass burning (BBN)	Biomass burning (BBN)
		Energy for buildings	Residential, commercial and other (RCO)
	Fossil fuels (FF)	Fuel exploitation (FUEL)	Energy transformation and extraction (ENE)
		Transport ^a	Surface transportation (TRA)
		Industry ^b	International shipping (SHP)
	Wetlands (WL)	Wetlands (WTL)	
Other sources (OT)	Agricultural waste burning	/	
	Geological seeps (SEE)		
	Termites (TER)		
Sinks	Soil uptake (SU)	Soil absorption (SAB)	
	Chemical loss (CL)	Tropospheric OH (OL)	
		Stratospheric loss (SL)	
		Tropospheric Cl (Cl)	

^a The transport source includes CH₄ emissions from aviation climbing, descent, cruise, landing, take off and supersonic, railways, pipelines, off-road transport, shipping, and road transportation.

^b The industry source includes emissions from oil refineries and transformation industry, power industry, combustion for manufacturing, chemical process, and iron and steel production.



20 **Figure S1.** Global mean tropospheric OH concentrations in 1980–2010 from the CESM model results of Zhao et al. (2019). OH concentrations are fixed to the 2010 levels for the years 2011–2018. The shading denotes $\pm 10\%$ of the prescribed OH levels in the sensitivity simulations (Table 1) for 2010–2018. The dashed black line represents the prescribed value of 10.6×10^5 molecules cm^{-3} (see Table 1).

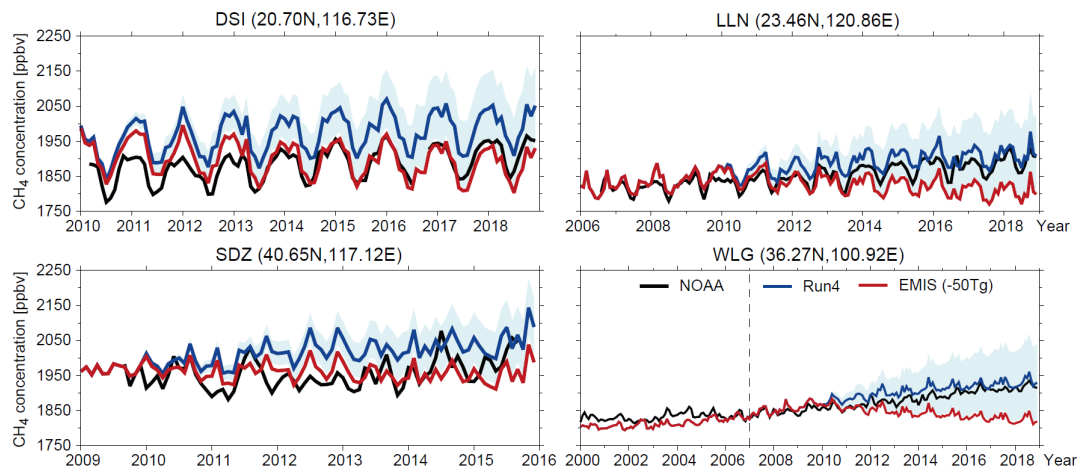


Figure S2. The influences of CH₄ emissions and OH levels on simulated CH₄ mixing ratios at Chinese surface sites. Measured monthly mean CH₄ mixing ratios at the four Chinese surface sites are compared with model results from the Run4 (with varying OH, blue lines) and Run7 (-50 Tg over 2010–2018, red lines) simulations (see Table 1). The blue shaded areas represent model results covered by ±10% of the prescribed OH levels in 2010-2018 (Run5 and Run6 in Table 1).

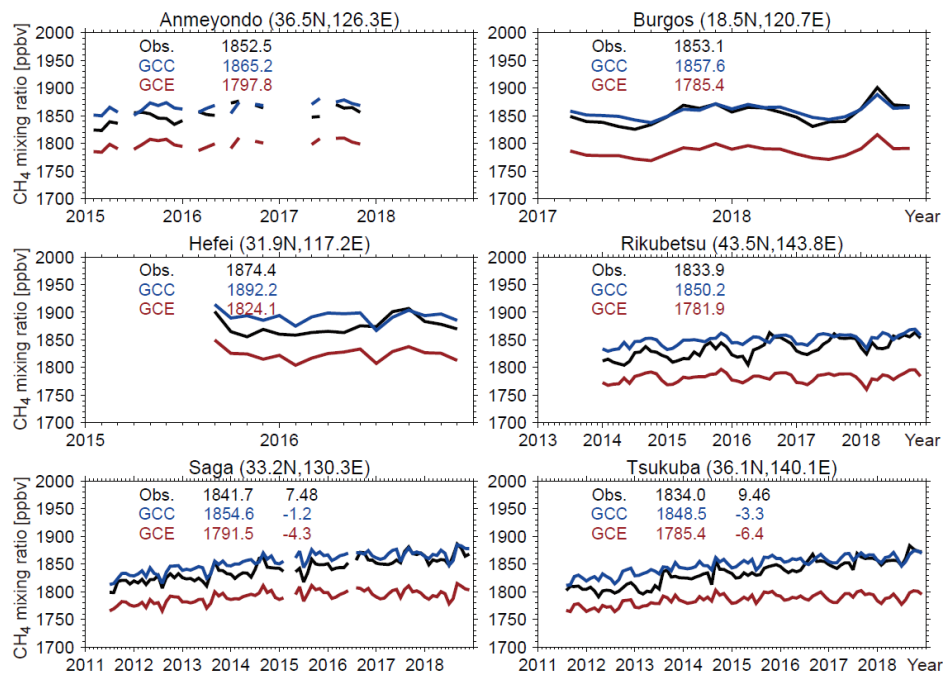
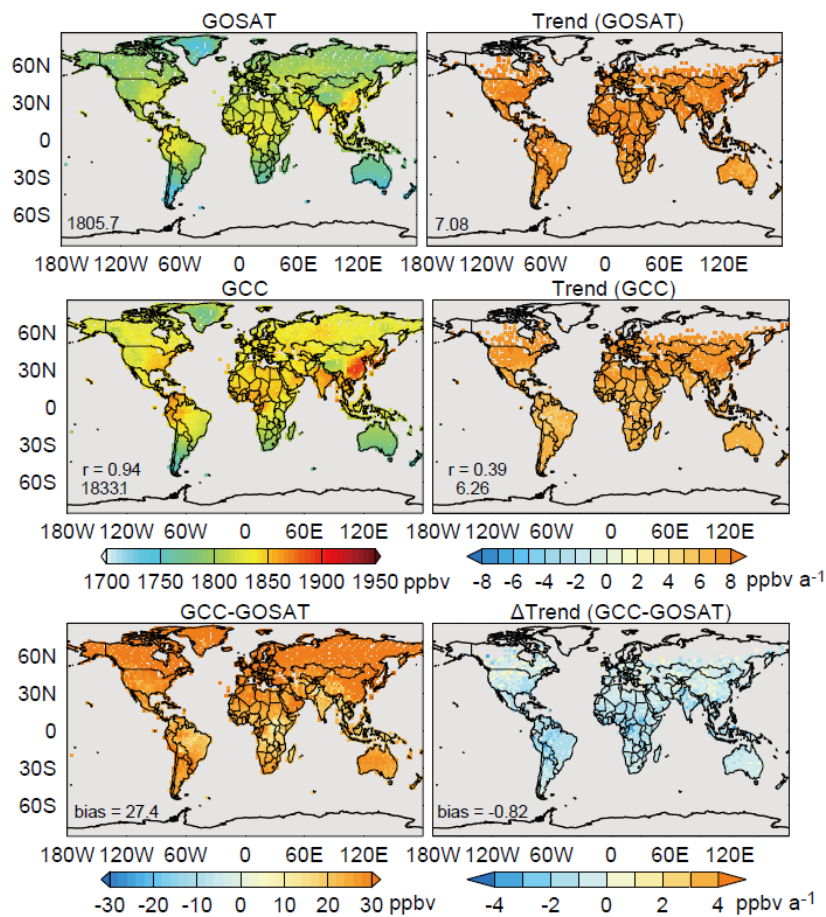
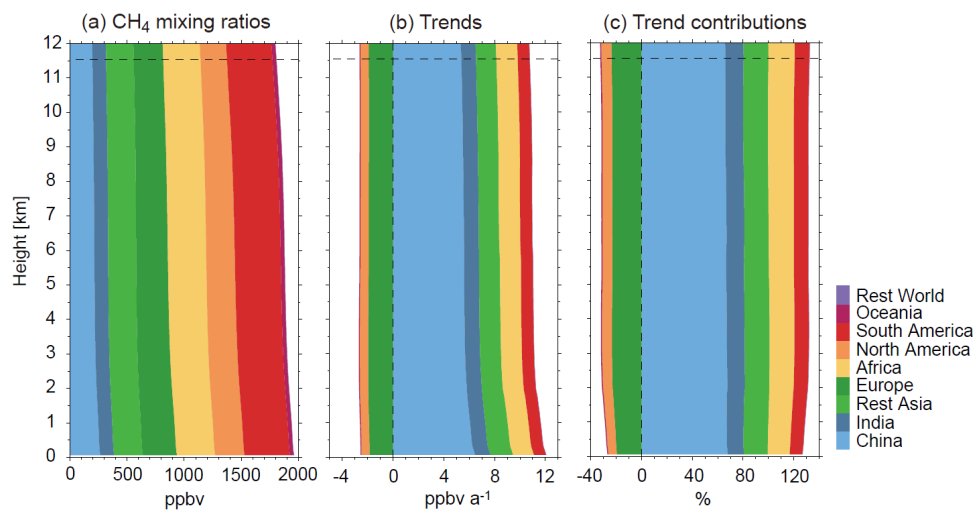


Figure S3. Comparison of GCE (red lines) and GCC (blue lines) simulated monthly results with TCCON observations of column CH_4 mixing ratios (black lines) in Asia. The observed mean mixing ratios (ppbv), trends (ppbv a^{-1}), and corresponding model biases are shown inset. Locations of the six measurement sites are shown in Fig. 1.



45 **Figure S4.** 2010–2017 annual mean GOSAT observed (top panels) and GCC model simulated (middle panels) atmospheric column mean CH_4 mixing ratios and trends. The bottom panels show model minus GOSAT differences.



55 **Figure S5.** Vertical distributions of Chinese (a) CH₄ mixing ratios, (b) trends and (c) trends in percentage as contributed by different region-specific tracers averaged over 2007–2018. Dashed lines denote the annual mean tropopause height over China.